

Quantitative Structure–Activity Relationship Modeling of Dopamine D₁ Antagonists Using Comparative Molecular Field Analysis, Genetic Algorithms–Partial Least-Squares, and K Nearest Neighbor Methods

Brian Hoffman,[†] Sung Jin Cho,[†] Weifan Zheng,[†] Steven Wyrick,[†] David E. Nichols,[§] Richard B. Mailman,^{*,†,‡} and Alexander Tropsha^{*,†}

Division of Medicinal Chemistry and Natural Products, School of Pharmacy, and Departments of Psychiatry and Pharmacology, University of North Carolina, Chapel Hill, North Carolina 27599, and Department of Medicinal Chemistry and Molecular Pharmacology, School of Pharmacy, Purdue University, West Lafayette, Indiana 47907

Received July 13, 1998

Several quantitative structure–activity relationship (QSAR) methods were applied to 29 chemically diverse D₁ dopamine antagonists. In addition to conventional 3D comparative molecular field analysis (CoMFA), cross-validated R^2 guided region selection (q^2 -GRS) CoMFA (see ref 1) was employed, as were two novel variable selection QSAR methods recently developed in one of our laboratories. These latter methods included genetic algorithm–partial least squares (GA–PLS) and K nearest neighbor (KNN) procedures (see refs 2–4), which utilize 2D topological descriptors of chemical structures. Each QSAR approach resulted in a highly predictive model, with cross-validated R^2 (q^2) values of 0.57 for CoMFA, 0.54 for q^2 -GRS, 0.73 for GA–PLS, and 0.79 for KNN. The success of all of the QSAR methods indicates the presence of an intrinsic structure–activity relationship in this group of compounds and affords more robust design and prediction of biological activities of novel D₁ ligands.

Introduction

The G protein-coupled receptor superfamily class includes the D₁-like and D₂-like dopamine receptors.⁵ Because dopamine neurotransmission is important in many aspects of CNS function (e.g., the modulation of motor activity and emotional states^{6,7}), it is not surprising that dopamine receptors play a role in the therapy and, possibly, the etiology of disorders such as Parkinson's disease and schizophrenia.⁸ For these reasons, there has been a great interest in studies aimed at mechanistic and functional understanding of dopamine receptor pharmacology. Despite the pace of advances in molecular and pharmacological knowledge of dopamine receptors, their X-ray crystallographic structure is not available. Thus, there is a particular need to develop molecular models that could help to both understand pharmacological data and predict novel biologically active compounds. Ligand-based methods of analysis, such as pharmacophore mapping and quantitative structure–activity relationships (QSAR), remain the major approach for developing predictive correlations between ligand structure and activity.

Recent modeling studies of dopaminergic ligands by us and other research groups have yielded several pharmacophore and QSAR models for a limited number of D₁ agonists^{9,10} and antagonists^{11,12} (recently reviewed¹³). The two literature accounts that address the QSAR of D₁ antagonists^{11,12} report the use of conventional regression analysis and CoMFA (comparative molecular field analysis) to develop a D₁ antagonist

model of binding affinity. The first of these studies (Charifson et al.¹¹) detailed the conformational studies and multiple linear regression (MLR) QSAR for a series of seven 1-phenyltetrahydroisoquinolines, compounds synthesized as ring-contracted analogues of the prototypical D₁ antagonist SCH23390. These analogues, although slightly lower in affinity, served as important probes of the D₁ antagonist pharmacophore, as they were useful in confirming the stereochemistry of the active site and provided variation in the 3D distribution of the pharmacophoric elements. Using the calculated dipole moment orientations of these ligands, a MLR QSAR model with a r^2 value of 0.95 was reported,¹¹ whereas models utilizing pharmacophoric atom distance comparisons yielded less favorable results.

The second literature report of D₁ antagonist QSAR (Minor et al.¹²) extended the work of Charifson et al. via the incorporation of additional tetrahydroisoquinoline (TIQ) analogues. Addition of five such TIQs to the MLR QSAR model of Charifson et al. resulted in a dramatic decrease in the correlation coefficient ($r^2 = 0.22$), indicating the limitations of this QSAR method. Inclusion of a second regressor, in the form of the torsion angle of the accessory phenyl ring bond, significantly enhanced the correlation, with an r^2 value of 0.92. Minor et al.¹² also reported the application of a 3D QSAR approach that made use of the field fit option of CoMFA for the analysis of a data set composed of 11 compounds. The resultant poor q^2 value (0.16) from this alignment method prompted the researchers to incorporate the torsion angle of the accessory phenyl ring bond as a regressor variable, as had been used in the development of the conventional QSAR analysis. This multiple regressor approach was more successful, with a q^2 of 0.578.

* To whom correspondence should be addressed.

[†] Division of Medicinal Chemistry and Natural Products.

[‡] Departments of Psychiatry and Pharmacology.

[§] Department of Medicinal Chemistry and Molecular Pharmacology.

The integrity and predictive power of such models improve with the use of more extensive training sets and the development of alternative QSAR models. Ideally, the compounds comprising the model should be numerous and of various structural classes. It is especially desirable that biological data used as the dependent variable be extremely reliable, i.e., derived within one laboratory utilizing sound experimental techniques. Furthermore, various QSAR models have the common purpose of establishing meaningful correlations between activity and quantitative descriptors of chemical structures. Thus, the successful development of alternative QSAR models confirms the existence of a structure–activity relationship intrinsic to a data set.

Several QSAR approaches have been developed over the years. Rapid accumulation of experimental 3D structural information about organic molecules of biological interest,^{14,15} paralleled by the more recent development of fast and accurate methods for 3D structure generation (e.g., CONCORD^{16,17}) and alignment (e.g., Active Analogue Approach^{18,19}), has led to the development of 3D structural descriptors and associated 3D QSAR methods. The examples of such descriptors include 3D shape descriptors used in molecular shape analysis,^{20,21} steric and electrostatic field sampling implemented in CoMFA,²² and comparative molecular similarity indices analysis (CoMSIA)²³ (several recent reviews on 3D QSAR have been published²⁴). One common characteristic of these methods, as opposed to traditional QSAR, is a dramatic increase in the number of descriptors. As this number increases, multiple regression methods become inadequate. Advances in chemometrics (e.g., principal component analysis²⁵ and partial least-squares^{22–26}) and machine learning algorithms (e.g., neural network^{27,28}), however, have provided researchers with adequate statistical tools to deal with this problem.

Reasonable simplicity, a high degree of automation, and a clear physicochemical sense of steric and electrostatic descriptors have made CoMFA one of the most popular methods for QSAR.²⁹ However, despite many successful applications, several problems have persisted with this method. For instance, we have shown recently that the results of conventional CoMFA may often be nonreproducible due to a sometimes-strong dependence of the CoMFA cross-validated correlation coefficient, q^2 , on the orientation of rigidly aligned molecules on the users' terminal.¹ We have offered a solution to this problem^{1,30} by developing a q^2 -guided region selection (q^2 -GRS) method that is based on rational selection of only the most significant regions of steric and electrostatic fields of aligned molecules. Nevertheless, especially for structurally diverse molecules, unambiguous 3D alignment in order to initiate the CoMFA process frequently remains a difficult task. In some reported cases, only the knowledge of 3D receptor structure has enabled the effective application of CoMFA.^{31,32}

The obvious difficulties with 3D alignment typical for 3D QSAR methods motivated us, as well as other researchers,³³ to consider possible alternatives that would combine the simplicity of 2D QSAR with the powerful statistical methods employed in 3D QSAR. To this end, we have considered the use of multiple 2D descriptors of chemical structures, such as topological

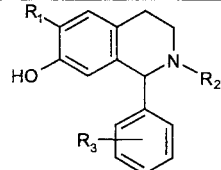
indices, that have been developed on the basis of chemical graph theory.^{34,35} Furthermore, we have implemented the concept of variable selection in QSAR, a process that has been explored recently by a number of researchers^{36,37} using such optimization methods as evolutionary algorithms,^{38,39} genetic algorithms,^{40,41} and simulated annealing algorithms.^{42,43} These considerations led us to develop two variable selection QSAR algorithms: genetic algorithm–partial least-squares (GA–PLS)^{3,4} and K nearest neighbor (KNN)^{2,4} analyses. These approaches currently rely upon topological descriptors of chemical structures that eliminate the conformational and alignment ambiguities inherent within the CoMFA process. Additionally, they are less computationally intensive and are practically automated. They have been used to produce highly predictive models^{2,3} that were comparable to, or better than, those obtained with traditional CoMFA.

In this paper, we have applied several QSAR approaches, including CoMFA, q^2 -GRS/CoMFA, GA–PLS, and KNN, to a data set of 29 structurally diverse D₁ antagonists. We measured the biological activity of all antagonists in rat striatal tissue. To the best of our knowledge, this is the most extensive and diverse set of D₁ antagonists studied experimentally in one laboratory. The purpose of this multiple QSAR analysis was both to test, in comparison, the efficiency of 2D vs 3D QSAR methods and to establish robust QSAR models for these ligands that can be used in the design of new high-affinity antagonists. In the case of 3D QSAR methods, i.e., CoMFA and q^2 -GRS, the Active Analogue Approach was applied for identification of the active pharmacophore in the alignment process. All four methods led to comparable QSAR models with cross-validated R^2 (q^2) values of 0.57 for CoMFA, 0.54 for q^2 -GRS, 0.73 for GA–PLS, and 0.79 for KNN.

Methods

Biological Activity Data. For this work, we have selected 29 chemically diverse D₁ dopamine antagonists (Tables 1–3) whose receptor affinity was measured in our laboratory. This data set includes a variety of tetrahydroisoquinolines (Tables 1 and 2), tetrahydrobenzazepines (Table 2), and phenylaminotetralins (Table 2), as well as representatives of several other series. The competition binding activity of the compounds is expressed as $-\log(K_{0.5})$ (Tables 1–3). The $K_{0.5}$ for a compound is an “apparent” affinity constant that is not affected by experimental variables such as varied radioligand concentrations. It may be considered a “corrected IC₅₀”. In the case of racemic mixtures, the affinity of the active enantiomer was approximated by dividing the $K_{0.5}$ by 2, making the assumption that one enantiomer was significantly less active than the other. This assumption is likely to be valid, based on the available data with this receptor and compounds of the structural classes we have utilized. Thus, for those compounds for which an active isomer was not known, there was extensive data on the absolute configuration of many close analogues. For instance, the active configuration of every 1-phenyltetrahydrobenzazepine that has been resolved is identical.^{44–46} Similarly, the active configuration of every 1-phenyltetrahydroisoquinoline is also identical, although opposite from that of the 1-phenyltetrahydrobenzazepines.^{11,12} Finally, the hypothesis of a single active isomer was confirmed by the recent analysis of the novel D₁ ligand dinapsoline.⁴⁷ Thus, modeling these analogues using this assumption is not based on conjecture alone.

Radioreceptor Assays. Adult male Sprague–Dawley rats were decapitated, and the corpus striatum was removed.

Table 1. Comparison of Different QSAR Methods as Applied to Compounds 1–11 of the 29 D₁ Antagonists Studied


ID	R ₁	R ₂	R ₃	Actual activity (-logK _{0.5})	Predicted activity KNN	Predicted activity GA-PLS	Fitted predicted activity CoMFA	Fitted predicted activity q ² -GRS CoMFA
1	Cl	CH ₃	H	8.28	7.51	7.69	8.04	7.75
2	Cl	CH ₃	<i>o</i> -CH ₃	8.43	8.34	8.29	8.23	8.27
3	Cl	CH ₃	<i>m</i> -CH ₃	8.38	8.34	8.25	8.28	8.26
4	Cl	CH ₃	<i>p</i> -CH ₃	8.28	8.40	8.13	7.92	8.33
5	Cl	CH ₃	<i>o</i> -CH(CH ₃) ₂	8.56	8.21	8.38	8.71	8.35
6	Cl	CH ₃	<i>o,o</i> -di-CH ₃	8.43	8.28	8.80	8.18	8.50
7	Cl	CH ₃	<i>o,m</i> -di CH ₃	8.00	7.67	8.49	8.42	8.41
8	Cl	CH ₃	<i>o</i> -Cl	8.43	8.34	8.56	8.51	8.48
9	Cl	propyl	H	7.05	7.60	7.15	7.31	7.80
10	H	CH ₃	H	6.37	8.49	6.28	6.33	7.85
11	Br	CH ₃	H	7.97	7.76	7.41	7.90	7.93

Striatal tissue was frozen immediately on dry ice and stored at -80 °C until needed. Homogenization of the tissue was effected in 50 mM HEPES buffer at pH 7.4 (25 °C) by seven manual strokes in a Wheaton Teflon-glass homogenizer. The tissue suspension was centrifuged at 27000g for 10 min, and the supernatant was discarded. This wash step was repeated once. The final pellet was resuspended at 1.25 mg/mL buffer. Binding was performed in 12- × 75-mm culture tubes at a volume of 1.0 mL. Each tube contained 800 μL of tissue homogenate suspension, 100 μL of the competing ligand solution, and 100 μL of the radioligand solution. Competing ligands were dissolved in methanol at a concentration of 1.0 mM and diluted with buffer to the appropriate concentrations. [³H]SCH23390 was diluted from a methanol stock solution to give a final incubation concentration of 0.25 nM. Nonspecific binding was defined with unlabeled SCH23390 (1 μM). Binding was terminated by rapid filtration with 15 mL of ice-cold buffer on a Skatron cell harvester using glass fiber filter mats. Following drying of the filters, 2–4 mL of Scintiverse E fluid was added. After agitation for 30 min, radioactivity was measured by scintillation analysis.

Most compounds (Tables 1–3) were either synthesized in our laboratories or obtained from commercial sources. Other compounds included SCH39166 (compound **26**), a generous gift of Schering-Plough, Inc., and the *N*-substituted analogues of SCH23390 (compounds **13–16**), provided by the Division of Intramural Research, National Institute on Drug Abuse, Baltimore, MD.

Synthesis. In addition to existing antagonists, several novel compounds were synthesized and included in the data set (compounds **2–8**). These compounds, 1-phenyltetrahydroisoquinolines, represent ring-contracted analogues of the 1-phenyltetrahydrobenzazepine SCH23390 and possess accessory phenyl ring substituents. The synthesis of these ligands followed the scheme of Charifson¹¹ utilizing an appropriate substituted benzoyl chloride. Scheme 1 outlines this general synthesis, while Table 4 lists relevant analytical data for these novel compounds.

Conventional CoMFA. Structures were generated and CoMFA was performed within the QSAR module of the SYBYL molecular modeling software.⁴⁸ Default Sybyl settings were used except as otherwise noted. Molecular mechanics calculations were performed with the standard Tripos force field, with a convergence criterion requiring a minimum energy change of 0.05 kcal/mol. Charges were calculated using the Delre method as implemented in SYBYL. The steric and electrostatic

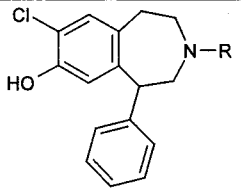
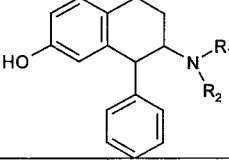
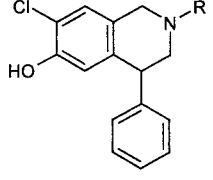
field energies were calculated using sp³ carbon probe atoms with a +1 charge. Low-energy conformers were obtained via the SYBYL random search method. The CoMFA QSAR equations were calculated using the partial least-squares (PLS) algorithm. The optimal number of components (ONC) in the final PLS model was determined by the cross-validated *R*² (*q*²) and standard error of prediction (SDEP) values, as obtained from the leave-one-out cross-validation technique. The *q*² value was calculated from the following standard equation:

$$q^2 = 1 - \frac{\sum (y_i - \bar{y})^2}{\sum (y_i - \hat{y}_i)^2} \quad (1)$$

in which *y_i* and *ŷ_i* are the actual activity and the predicted activity of the *i*th compound, respectively, and *ȳ* is the average activity of all the compounds in the training set. Both summations are inclusive of all compounds in the training set. The number of components with the lowest SDEP value was selected as the ONC. All calculations were performed on a Silicon Graphics Indigo² workstation.

Structure Alignment. This section describes the methodology employed only in the cases of CoMFA and *q*²-GRS, since these methods require rational 3D alignment of the database molecules for generation of the descriptors. We have utilized the protonated forms of the compounds, as it has been well-established that the nitrogens would exist mainly in the protonated form at physiological pH⁴⁹ and all ligands that are known to bind to dopamine receptors possess an amino function with a p*K_a* greater than 7.⁵⁰ The geometry of each antagonist was optimized individually with the Tripos force field, with no constraints on the internal geometry of the molecules. Compound **26** (SCH39166), a ring-constrained analogue of compound **12** (SCH23390), was chosen as the template molecule due to its rigidity and relatively high affinity. The conformations of compound **12** and the template antagonist **26** were based on their published⁵¹ X-ray crystal structures. Additional X-ray crystal structures were obtained from the Cambridge Structural Database, including those for compounds **28** and **29**. The conformation of compounds **1** and **24** that were utilized in our model have also been described previously,^{11,12} as have the conformations of *N*-methyl-substituted compounds **13–16**.⁵² Compound **25** was modeled in the half-chair conformation of tetrahydroisoquinolines described by Charifson et al.; however, in the absence of

Table 2. Comparison of Different QSAR Methods as Applied to Compounds 12–23 of the 29 D₁ Antagonists Studied

ID			Actual activity	Predicted activity	Predicted activity	Fitted predicted activity	Fitted predicted activity
	R		(-logK _{0.5})	KNN	GA-PLS	CoMFA	q ² -GRS CoMFA
12	CH ₃		9.40	9.49	8.02	9.04	7.91
13	(CH ₂) ₆ NHCH ₃		6.86	7.54	6.49	6.82	7.13
14	(CH ₂) ₆ N(CH ₃) ₂		6.94	7.18	7.24	6.97	7.22
15	(CH ₂) ₂ C ₆ H ₄ -o-N(CH ₃) ₂		7.43	7.14	7.39	7.58	5.74
16	CH=CHC ₆ H ₄ -o-N(CH ₃) ₂		7.54	7.24	7.56	7.51	6.94
							
ID	R ₁	R ₂	Actual activity	Predicted activity	Predicted activity	Fitted predicted activity	Fitted predicted activity
			(-logK _{0.5})	KNN	GA-PLS	CoMFA	q ² -GRS CoMFA
17	H	H	5.53	5.95	5.77	5.80	5.30
18	H	CH ₃	5.46	7.76	5.61	5.65	5.72
19	CH ₃	CH ₃	5.85	5.91	6.42	6.12	5.71
20	H	(CH ₂) ₂ CH ₃	6.02	5.64	5.63	5.74	5.86
21	CH ₃	(CH ₂) ₂ CH ₃	5.82	5.93	5.97	5.63	6.19
ID			Actual activity	Predicted activity	Predicted activity	Fitted predicted activity	Fitted predicted activity
	R		(-logK _{0.5})	KNN ^a	GA-PLS ^b	CoMFA ^c	q ² -GRS CoMFA ^d
	22	H		6.55	7.18	6.92	6.42
23	CH ₃		7.06	7.15	7.95	7.08	6.65

conformational data regarding the probable orientation of the accessory benzyl ring (as exists for the accessory phenyl ring of compounds **1**¹¹ and **12**),^{53,54} we modified the torsion angle of the benzyl group to mimic the phenyl ring position of the template molecule **26**. For compounds **17–21**, the chosen conformation of compound **24** was utilized, with the deletion and addition of appropriate atoms, followed by geometry optimization as described above. This procedure was also used in defining the conformation of compound **27**. The appropriate conformations of compounds **22** and **23** were determined by deletion and addition of appropriate atoms of the chosen conformation of compound **1**, geometry optimization as described above, and a subsequent random search using Sybyl default values (except "check chirality", set to preserve the stereochemistry of the molecule). This random search yielded two conformer candidates, with energy values of 9.88 and 10.53 kcal/mol, and the conformer with the lower energy value was retained for alignment.

Pharmacophore Assignment. Structural alignment for CoMFA and q²-GRS is dependent upon a rational identification of the pharmacophore of each compound in the data set. The alignment of our data set is illustrated in Figure 1. For this process of pharmacophore assignment, we followed our previously developed model of the D₁ receptor active site that was obtained with the Active Analogue Approach.¹⁹ According to that model, the pharmacophore of the tetrahydroisoquinolines (compounds **1–11**, **22–25**) and tetrahydrobenzazepines (com-

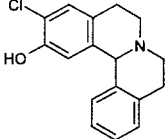
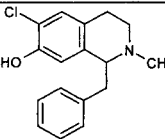
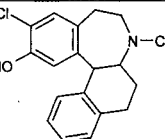
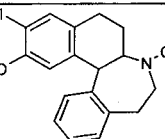
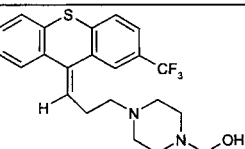
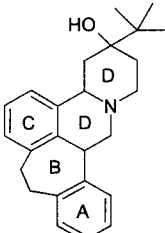
pounds **12–16**, **26**) consists of the chlorine (or other halogen in some molecules), the hydroxyl group oxygen (O.3), the quaternary nitrogen (N.4), and the centroid of the accessory phenyl ring. The following alignment rules were utilized for antagonists that were neither tetrahydrobenzazepines nor tetrahydroisoquinolines.

1. Compounds **17–21**, phenylaminotetralin analogues, were aligned using the oxygen (O.3) of their hydroxyl groups (fit to the oxygen of the template molecule), their secondary, tertiary, or quaternary nitrogen (fit to the quaternary nitrogen of the template), the 6-position hydrogen (fit to the chlorine of the template molecule), and the centroid of their accessory phenyl rings (fit to the centroid of the accessory phenyl ring of the template).

2. Compound **27**, a fused-ring phenylaminotetralin analogue, was aligned by its iodine substituent (fit to the chlorine of the template), the hydroxyl group oxygen (O.3) (fit to the oxygen of the hydroxyl group of the template), the quaternary nitrogen (N.4) (fit to the quaternary nitrogen of the template), and the centroid of the accessory phenyl ring (fit to the centroid of the accessory phenyl ring of the template).

3. Compound **28**, flupenthixol, was aligned by the centroid of the substituted phenyl ring (fit to the fused ring of the template), the centroid of the second phenyl ring (fit to the centroid of the accessory phenyl ring of the template), and the tertiary nitrogen (N.3) (fit to the quaternary nitrogen of the template).

Table 3. Comparison of Different QSAR Methods as Applied to Compounds 24–29 of the 29 D₁ Antagonists Studied

ID	Compound structure	Actual activity (-logK _{0.5})	Predicted activity KNN	Predicted activity GA-PLS	Fitted predicted activity CoMFA	Fitted predicted activity q ² -GRS CoMFA
24		5.68	6.80	6.66	5.93	7.03
25		7.24	6.80	7.52	7.71	7.09
26		8.30	7.76	6.97	8.67	7.93
27		5.96	6.99	5.92	5.58	6.92
28		7.97	7.49	8.10	7.45	6.07
29		9.00	7.86	9.20	8.93	7.08

4. Compound **29**, butaclamol, was oriented using the centroid of ring C (fit to the fused phenyl ring of the template molecule), the centroid of ring A (fit to the centroid of the accessory phenyl ring of the template), and the tertiary nitrogen (N.3) (fit to the quaternary nitrogen of the template).

q²-GRS Routine. The q²-GRS process has been described in detail elsewhere^{1,30} (see also recent review⁵⁵). Unlike conventional CoMFA, the q²-GRS method leads to reproducible q² values that do not depend on the orientation of a molecular aggregate of aligned molecules on the user terminal.¹ The q²-GRS procedure is as follows: **Step 1.** Conventional CoMFA is performed using the automatically generated region file (a rectangular grid). **Step 2.** The rectangular grid, encompassing the aligned molecules, is divided into 125 small boxes of equal size. **Step 3.** For each of these newly generated subregion files, a separate CoMFA is performed, with a step size of 1.0 Å. **Step 4.** The regions possessing a q² value greater than the specified threshold value are selected for further analysis. **Step 5.** The selected regions are combined to generate a master region file. **Step 6.** The final CoMFA is performed using the master region file.

GA-PLS Routine. The algorithm of the GA-PLS method^{3,4} is implemented as follows: **Step 1.** The Molconn-X program⁵⁶ is applied to generate 462 variables (topological indices) automatically. **Step 2.** All atom id-dependent descriptors (150

descriptors) and descriptors with zero variance are removed (the atom id-dependent indices are eliminated because atom ids are assigned arbitrarily and variations in these indices do not reflect any structural changes). **Step 3.** All applicable descriptors are numbered arbitrarily, and this enumeration is maintained throughout the entire analysis. A population of 100 different random combinations of these descriptors is generated. To apply GA methodology, each combination is considered as a parent. Each parent represents a binary string of digits, either "1" or "0"; the length of each string is the same and is equal to the total number of descriptors (indices). The value of "1" implies that the corresponding descriptor is included for the parent, and "0" means that the descriptor is excluded. **Step 4.** Using each parent combination of descriptors, a QSAR equation is generated for the whole data set using the PLS algorithm; thus for each parent an initial value of q² is obtained. The [1 - (n - 1)(1 - q²)/(n - c)] expression (in which q² is cross-validated R², n is the number of compounds, and c is the optimal number of components) then is used as the fitting function to guide the GA optimization. **Step 5.** Two parents are selected randomly based on the roulette wheel selection method. **Step 6.** The population is evolved by performing a crossover between two randomly selected parents, producing two offspring. **Step 7.** Each offspring is subjected to a random single-point mutation, i.e., a randomly

Scheme 1. Synthesis of Novel Substituted 1-Phenyltetrahydroisoquinolines

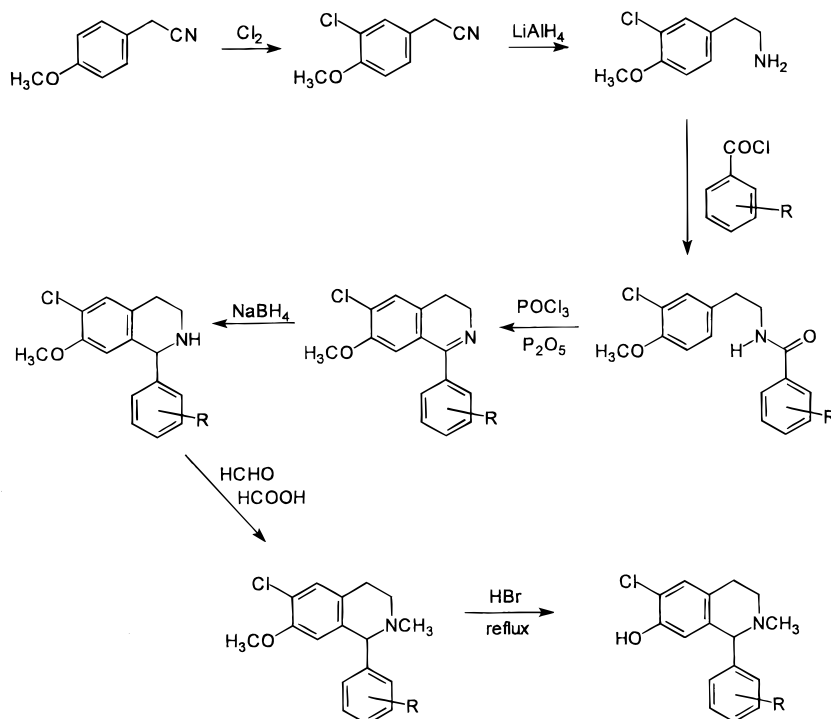
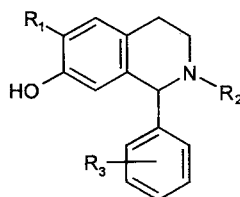


Table 4. Analytical Data for Novel Phenyl-Substituted Tetrahydroisoquinolines



ID	R ₁	R ₂	R ₃	Melting point (°C)	Combustion analysis	
					Calculated	Found
2	Cl	CH ₃	<i>o</i> -CH ₃	61-63, with decomposition	C: 70.98 H: 6.26	C: 71.10 H: 6.28
3	Cl	CH ₃	<i>m</i> -CH ₃	270, with decomposition	C: 70.98 H: 6.26	C: 71.06 H: 6.35
4	Cl	CH ₃	<i>p</i> -CH ₃	169-171 (with decomposition)	C: 70.98 H: 6.26	C: 70.85 H: 6.39
5	Cl	CH ₃	<i>o</i> -CH(CH ₃) ₂	59-61, with decomposition	C: 72.29 H: 6.97	C: 72.40 H: 6.99
6	Cl	CH ₃	<i>o,o</i> -di-CH ₃	51-52, with decomposition	C: 71.66 H: 6.63	C: 71.91 H: 6.53
7	Cl	CH ₃	<i>o,m</i> -di-CH ₃	155-156, with decomposition	C: 71.66 H: 6.63	C: 71.60 H: 6.46
8	Cl	CH ₃	<i>o</i> -Cl	106-107	C: 62.38 H: 4.87	C: 62.21 H: 4.99

selected "1" (or "0") is changed to "0" (or "1"). **Step 8.** The fitness of each offspring is evaluated as described above (cf. step 4). **Step 9.** If the resulting offspring are characterized by a higher value of the fitness function, then they replace less fit parents; otherwise, the parents are kept. **Step 10.** Steps 5–9 are repeated until a predefined maximum number of crossovers are reached.

KNN Routine. The essential aspects of this method^{2,4} are as follows: All compounds are initially described by multiple descriptors, i.e., topological indices calculated with the MOL-

CON-X program.⁵⁶ The activity of each compound is predicted as the average of two (or K in the general case) most similar compounds in the data set; the similarity is determined by the Euclidean distance between a pair of compounds in multi-dimensional descriptor space. The search in the descriptor space to select the best subset of variables (variable selection) is performed using stochastic algorithms (simulated annealing or genetic algorithms). The search continues until it converges to the subset of descriptors that afford the highest q^2 value. The further details of this method are described elsewhere.^{2,4}

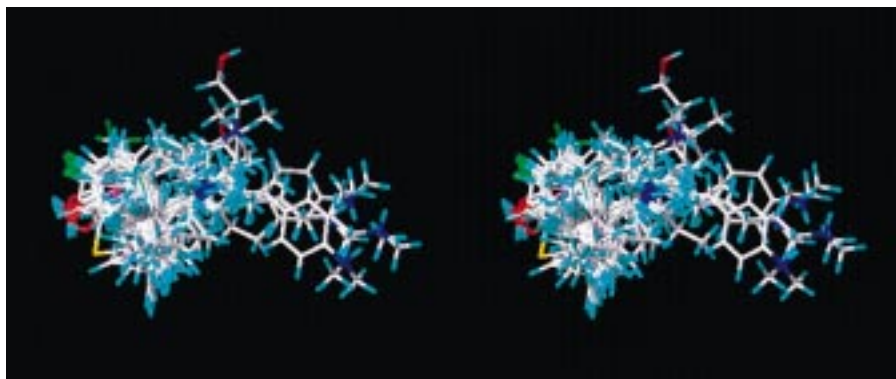


Figure 1. Stereoview of the 29 aligned D₁ antagonists utilized in this study.

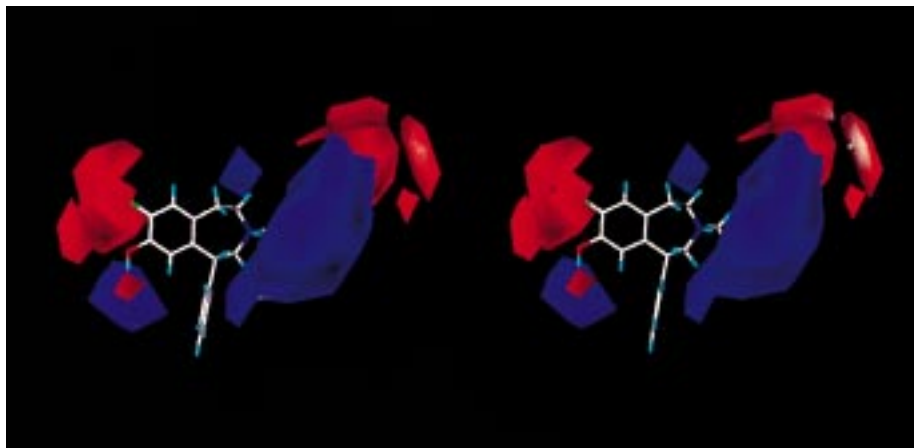


Figure 2. Stereoview of the electrostatic fields generated with CoMFA, with SCH23390 as a representative ligand: blue indicates regions where binding is possibly improved by more positively charged substituents; red indicates regions where binding is possibly improved by more negatively charged substituents.

Results and Discussion

Tables 1–3 list predicted vs actual biological values for each compound, as determined by each type of QSAR analysis. The use of biological data from one source is of particular significance, preventing interlaboratory variations in the values of dependent variable for the QSAR analysis. We discuss the results of each analysis separately *vide infra*.

QSAR Models Based on CoMFA. The use of our previously developed pharmacophore model¹⁹ for molecular alignment provided a rational foundation for the 3D QSAR analyses we report here. Compound **26** provided an appropriate template for alignment of the members of the data set in CoMFA and q^2 -GRS, given its high affinity and conformational rigidity. The results for q^2 -GRS were practically the same as for conventional CoMFA (cf. Tables 1–3). This may be due to fortuitously optimal orientation of the database molecules: the molecules may have been oriented on the user terminal in a manner that yielded the highest q^2 value possible. Another possibility is that the molecules of the data set possess structural features that translate into descriptors that are not improved by the region-selection procedure of the q^2 -GRS analysis. For example, although the data set consisted of several molecular classes of compounds, within each class there was little deviation in the pharmacophoric arrangement. Were there more variability within the data set with regard to the pharmacophore of each ligand, the advantage of region selection may have resulted in an improved q^2 value.

One or both of these possibilities may contribute to the lack of improvement by the q^2 -GRS analysis.

Figures 2 and 3 illustrate steric and electrostatic fields generated by CoMFA. These fields can be interpreted in terms of structural modifications that might improve binding affinity with changes in substituent charges and/or sizes. In each figure, SCH23390 (compound **12**) is the representative ligand displayed within the CoMFA fields. Figure 2 shows electrostatic fields, with blue regions indicative of areas, where, as predicted by CoMFA, the affinity might be improved by more positively charged substituents. Red regions are indicative of areas where the affinity might be improved by more negatively charged substituents. The red regions surrounding the 7-chloro substituent of SCH23390 may be representative of the observation that the binding affinities of D₁ ligands generally improve with 7-position substituents according to the following trend: I < H < Br ~ Cl, as observed in the 1-phenylbenzazepine series by Iorio et al.⁵⁷ and Tice et al.⁴⁶ This trend in affinity correlates with the electrostatic charges of the 7-position substituents. The blue region extending from the tertiary nitrogen of SCH23390 correlates to the position of the extended chain substituents seen in compounds **13**–**16**. While these compounds exhibited only modest affinity when tested in our laboratories, they had higher affinity than other extended *N*-substituted compounds, such as analogues **9**, **20**, and **21**.

Similarly, Figure 3 shows CoMFA steric fields. Yellow regions indicate areas where bulkier substituents lead

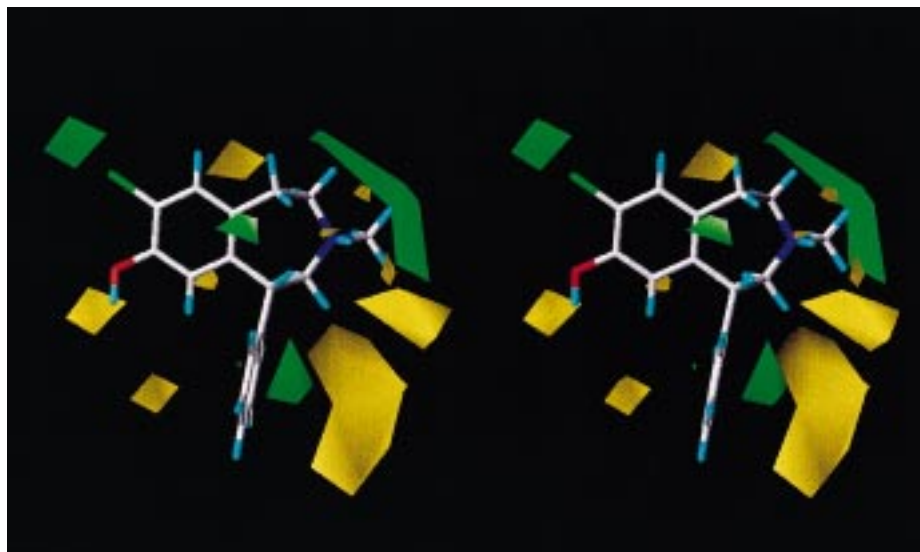


Figure 3. Stereoview of the steric fields generated with CoMFA, with SCH23390 as a representative ligand: yellow indicates regions of possible unfavorable steric interactions of bulky substituents with the receptor; green indicates regions where binding is possibly improved by bulky substituents.

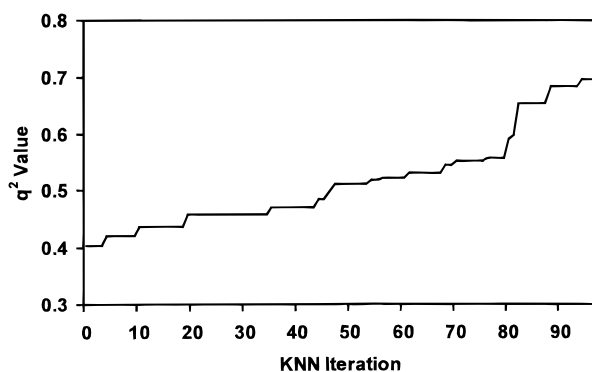


Figure 4. Trajectory of the SA-driven optimization of q^2 values in developing the KNN QSAR model for D₁ antagonists.

to the decrease in activity, and green regions are indicative of areas predicted by CoMFA to be improved by bulkier substituents. These fields are less pronounced than those illustrated for electrostatic fields in Figure 2. The yellow region at the bottom right corresponds to steric factors exhibited by the low-affinity ligands **24** and **27**. The green region proximal to the tertiary nitrogen appears to match van der Waals contributions from the extended chain substituents of compounds **13–16**.

QSAR Models Based on Topological Descriptors: Comparison with CoMFA. The trajectories of the q^2 values for KNN and GA-PLS QSAR methods in the course of the model optimization are shown in Figures 4 and 5, respectively. The final results obtained with GA-PLS and KNN methods are given in Table 5 as well. These methods, which utilize only 2D topological description of molecules, yielded q^2 values of 0.73 and 0.79 for GA-PLS and KNN calculations, respectively. Since all QSAR methods employed in this paper use the same criteria of the quality of the QSAR model, i.e., q^2 , the results of the methods can be compared directly. Apparently, the q^2 values obtained from GA-PLS and KNN QSAR methods are better than those from the 3D QSAR methods of CoMFA or q^2 -GRS (0.57 and 0.54, respectively).

These results demonstrate that both KNN and GA-PLS are highly competitive QSAR analytical techniques

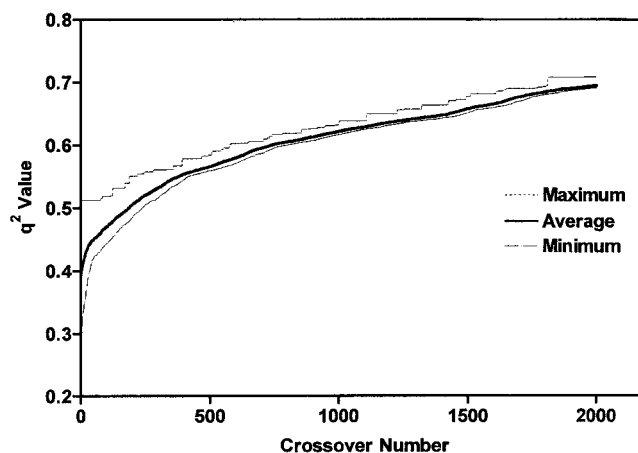


Figure 5. Trajectory of the GA-driven optimization of q^2 values for the GA-PLS QSAR model of D₁ antagonists.

as applied to this data set. Both methods have certain inherent advantages over 3D methods, such as circumvention of alignment issues as well as the elimination of the possibility of inappropriate conformation selection. Furthermore, they employ variable selection procedures that improve the quality of QSAR analysis, especially if the number of descriptors is large. The success of alignment-free QSAR methods utilizing 2D descriptors may also indicate that in the case of relatively rigid compounds such as D₁ antagonists, 2D description of the pharmacophore is sufficient to establish adequate structure-activity correlations.

The greater success of 2D QSAR methods notwithstanding, all four QSAR methods have yielded highly predictive models. The success of these models is noteworthy, since we have dealt with a large data set comprised of a variety of structural classes. Structural variations of the D₁ ligands included differing substituents of the accessory phenyl ring, differing positions and substitutions of the nitrogen, and differing substituents in the catechol ring.

We were curious to explore the contribution of the two non-catechol-like antagonists (compounds **28** and **29**) to our QSAR models. It is interesting to note that dropping

Table 5. Statistical Data for QSAR Method Results

Statistical value	QSAR method			
	KNN	GA-PLS	CoMFA	q ² -GRS-CoMFA
q ²	0.79	0.73	0.57	0.54
Optimal number of components	not applicable	4	5	7
Standard error of prediction	0.882	0.637	0.951	0.898
R ²	0.561	0.722	0.940	0.494
F value	22.99	21.66	79.75	2.090

these two antagonists from the data set increases the q^2 value for CoMFA from 0.57 to 0.72. In contrast, no appreciable difference in the q^2 value was observed with 2D QSAR approaches. On the basis of these observations, we have proposed that these "nontraditional" antagonists bind to the D₁ receptor in a different manner than traditional (benzazepine and isoquinoline) antagonists. Our preliminary receptor–ligand docking studies using a tentative 3D model of the D₁ receptor also support this hypothesis. We shall repeat CoMFA analysis for the whole data set using receptor-based alignment of all compounds once our receptor model has been refined. The lack of sensitivity of both GA–PLS and KNN methods to the presence or absence of these two compounds in the data set is not surprising, since neither 2D QSAR method relies upon compound alignment.

Conclusions and Prospectus

We have developed several QSAR models for 29 diverse antagonists of the D₁ receptor. Although these models are based on different QSAR protocols and different types of descriptors, they are all statistically valid as indicated by high q^2 values. The CoMFA fields generated from these studies predict improved affinity for compounds possessing positively charged substituents extending from the tertiary nitrogen common to dopaminergic antagonists. This prediction is in accord with previously reported data regarding the extended chain *N*-substituted compounds **13**–**16**,^{52,58} although these drugs possess lower affinity in our biological assays. The prediction that negatively charged substituents in the position analogous to the 7-position of SCH23390 would improve affinity is probably based on the rank order of affinity of various halogen-substituted compounds, with more negatively charged chlorine-substituted compounds more potent than iodinated or unsubstituted compounds. This prediction is not supported by literature accounts of binding affinity of a fluoro-substituted analogue of SCH23390, which has weaker affinity than chloro- and bromo-substituted analogues.⁵⁷

An interesting outcome of these QSAR studies is the observation that inclusion of two non-catechol antagonists, compounds **28** and **29**, lowers the q^2 values of the 3D QSAR analytical methods used here. When included in data sets, analyzed by KNN and GA–PLS methods, these compounds do not decrease q^2 values, likely because these QSAR methods do not rely upon alignment of members of the data sets. We have proposed that these antagonists **28** and **29** bind to the D₁ receptor in a manner that differs from catechol-like antagonists,

occupying part of the same binding region but probably interacting with different residues. This hypothesis is currently under investigation in our group using a 3D model of the D₁ receptor, and the results will be a subject of separate publication.

The relative success of QSAR approaches as divergent as those applied in this paper indicates the existence of an inherent quantitative structure–activity relationship for D₁ receptor ligands, which can be expressed using a variety of formal molecular descriptors and QSAR models. The concurrent use of these different models should significantly increase our confidence in the prediction of biological activity for newly designed compounds.

References

- (1) Cho, S. J.; Tropsha, A. Cross-Validated R² Guided Region Selection for Comparative Molecular Field Analysis (CoMFA): A Simple Method to Achieve Consistent Results. *J. Med. Chem.* **1995**, *38*, 1060–1066.
- (2) (a) Zheng, W.; Cho, S. J.; Tropsha, A. Novel computational tools for rational drug design using combinatorial chemistry and QSAR. *Books of Abstracts. 213th National Meeting, Las Vegas, NE, September 8–12, 1997*; American Chemical Society: Washington, DC. (b) Zheng, W.; Tropsha, A. Application of the K Nearest Neighbor with Variable Selection Method to QSAR. *J. Comput. Chem.*, accepted.
- (3) Cho, S. J.; Cummins, D.; Bentley, J.; Andrews, C. W.; Tropsha, A. Application of Genetic Algorithms and Partial Least Squares to Variable Selection of Topological Indices. *J. Comput.-Aided Mol. Des.*, submitted. (b) The method is described in detail and can be executed on the QSAR Web server available at <http://mmlin1.pha.unc.edu/~jin/QSAR>.
- (4) Tropsha, A.; Cho, S. J.; Zheng, W. "New Tricks for an Old Dog": Development and Application of Novel QSAR Methods for Rational Design of Combinatorial Chemical Libraries and Database Mining. *Rational Drug Design: Novel Methodology and Practical Applications*; ACS Symp. Series 719; American Chemical Society: Washington, DC, 1999, in press.
- (5) Keabian, J.; Calne, D. B. Multiple receptors for dopamine. *Nature* **1979**, *277*, 93–96.
- (6) Strange, P. G. *Brain Biochemistry and Brain Disorders*; Oxford University Press: New York, 1993.
- (7) Waddington, J. *D₁:D₂ Dopamine Receptor Interactions*; Academic Press: New York, 1993.
- (8) Seaman, P.; Bzowej, N. H.; Guan, H. C.; Bergeon, C.; Reynolds, G. P.; Bird, E. D.; Riederer, P.; Jellinger, K.; Tortellotte, W. W. Human brain D₁ and D₂ dopamine receptors in schizophrenia, Alzheimer's, Parkinson's, and Huntington's diseases. *Neuropsychopharmacology* **1987**, *1*, 5–15.
- (9) Mottola, D. M.; Laiter, S.; Watts, V. J.; Tropsha, A.; Wyrick, S. W.; Nichols, D. E.; Mailman, R. B. Conformational analysis of D₁ dopamine receptor agonists: pharmacophore assessment and receptor mapping. *J. Med. Chem.* **1996**, *39*, 285–296.
- (10) Brusnniak, M. K.; Pearlman, R. S.; Neve, K. A.; Wilcox, R. E. Comparative molecular field analysis-based prediction of drug affinities at recombinant D_{1A} dopamine receptors. *J. Med. Chem.* **1996**, *39*, 850–859.
- (11) Charifson, P. S.; Bowen, J. P.; Wyrick, S. D.; Hoffman, A. J.; Cory, M.; McPhail, A. T.; Mailman, R. B. Conformational analysis and molecular modeling of 1-phenyl-, 4-phenyl-, and 1-benzyl-1,2,3,4-tetrahydroisoquinolines as D₁ dopamine receptor ligands. *J. Med. Chem.* **1989**, *32*, 2050–2058.

- (12) Minor, D. L.; Wyrick, S. D.; Charifson, P. S.; Watts, V. J.; Nichols, D. E.; Mailman, R. B. Synthesis and molecular modeling of 1-phenyl-1,2,3,4-tetrahydroisoquinolines and related 5,6,8,9-tetrahydro-13bH-dibenzo[a,h]quinolizines as D₁ dopamine antagonists. *J. Med. Chem.* **1994**, *37*, 4317–4328.
- (13) Mailman, R. B.; Nichols, D. E.; Tropsha, A. Molecular Drug Design and Dopamine Receptors. In *Dopamine Receptors*, Neve, K., Neve, R., Eds.; Humana Press: Totowa, NJ, 1996; pp 105–133.
- (14) Allen, F. H.; Davies, J. E.; Galloy, J. J.; Johnson, O.; Kennard, O.; Macrae, C. F.; Mitchell, E. M.; Mitchell, G. F.; Smith, J. M.; Watson, D. G. The development of versions 3 and 4 of the Cambridge Structural Database System. *J. Chem. Inf. Comput. Sci.* **1991**, *31*, 187–204.
- (15) Allen, F. H.; Bellard, S.; Brice, M. D.; Cartwright, B. A.; Doubleday, A.; Higgs, H.; Hummelink, T.; Hummelink-Peters, B. G.; Kennard, O.; Motherwell, W. D. S.; Rodgers, J. R.; Watson, D. G. The Cambridge Crystal Data Centre: computer-based search, retrieval, analysis, and display of information. *Acta Crystallogr. Sect. B: Struct. Crystallogr. Cryst. Chem.* **1979**, *B35*, 2331–2339.
- (16) Rusinko, A., III; Skell, J. M.; Balducci, R.; McGarity, C. M.; Pearlman, R. S. *Concord, A Program for the Rapid Generation of High Quality Approximate 3-Dimensional Molecular Structures*; The University of Texas at Austin and Tripos Associates: St. Louis, MO, 1988.
- (17) Pearlman, R. S. Rapid generation of high quality approximate 3D molecular structures. *Chem. Des. Aut. News* **1987**, *2*, 1–6.
- (18) Marshall, G. R.; Barry, C. D.; Bosshard, H. E.; Dammkoehler, R. A.; Dunn, D. A. The Conformational Parameter in Drug Design: the Active Analogue Approach. In *Computer-Assisted Drug Design*; Olson, E. C., Christoffersen, R. E., Eds.; American Chemical Society, Washington, DC, 1979; Vol. 112, pp 205–226.
- (19) Marshall, G. R.; Cramer, R. D., III. Three-Dimensional Structure-Activity Relationships. *TIPS Rev.* **1988**, *9*, 285–289.
- (20) Simon, Z.; Badilescu, I.; Racovitan, T. Mapping of dihydrofolate-reductase receptor site by correlation with minimal topological (steric) differences. *J. Theor. Biol.* **1977**, *66*, 485–495.
- (21) Rhyu, K. B.; Patel, H. C.; Hopfinger, A. J. A 3D-QSAR Study of Anticoccidial Triazines using molecular shape analysis. *J. Chem. Inf. Comput. Sci.* **1995**, *35*, 771–778.
- (22) Cramer, R. D., III; Patterson, D. E.; Bunce, J. D. Comparative Molecular Field Analysis (CoMFA). 1. Effect of Shape on Binding of Steroids to Carrier Proteins. *J. Am. Chem. Soc.* **1988**, *110*, 5959–5967.
- (23) Klebe, G.; Abraham, U.; Mietzner, T. Molecular Similarity Indices in a Comparative Analysis (CoMSIA) of Drug Molecules to Correlate and Predict Their Biological Activity. *J. Med. Chem.* **1994**, *37*, 4130–4146.
- (24) Kubinyi, H.; Folkers, G.; Martyn, Y. *3D QSAR in Drug Design*; Kluwer/ESCOM: Leiden, 1998; Vol. 2–3.
- (25) Camilleri, P.; Livingstone, D. J.; Murphy, J. A.; Manallack, D. T. Chiral Chromatography and Multivariate Quantitative Structure–Property Relationships of Benzimidazole Sulphoxides. *J. Comput.-Aided Mol. Des.* **1993**, *7*, 61–69.
- (26) Geladi, P.; Kowalski, B. R. Partial Least Squares Regression: A Tutorial. *Anal. Chim. Acta* **1986**, *185*, 1–17.
- (27) Jansson, P. A. Neural Networks: An Overview. *Anal. Chem.* **1991**, *63*, 357A–362A.
- (28) So, S. S.; Richards, W. G. Application of Neural Networks: Quantitative Structure–Activity Relationships of the Derivatives of 2,4-Diamino-5-(substituted-benzy)pyrimidines as DHFR Inhibitors. *J. Med. Chem.* **1992**, *35*, 3201–3207.
- (29) Cramer, R. D., III; DePriest, S. A.; Patterson, D. E.; Hecht, P. The Developing Practice of Comparative Molecular Field Analysis. In *3D QSAR in Drug Design: Theory, Methods, and Applications*; Kubinyi, H., Ed.; ESCOM: Leiden, 1993; pp 443–485.
- (30) Cho, S. J.; Tropsha, A.; Suffness, M.; Cheng, Y. C.; Lee, K. H. Antitumor Agents. 163. Three-Dimensional Quantitative Structure–Activity Relationship Study of 4'-O-Demethylpiperidophylotoxin Analogues Using the Modified CoMFA/ q^2 -GRS Approach. *J. Med. Chem.* **1996**, *39*, 1383–1395.
- (31) Waller, C. L.; Oprea, T. I.; Giolitti, A.; Marshall, G. R. Three-Dimensional QSAR of Human Immunodeficiency Virus (I) Protease Inhibitors. 1. A CoMFA Study Employing Experimentally-Determined Alignment Rules. *J. Med. Chem.* **1993**, *36*, 4152–4160.
- (32) Cho, S. J.; Garsia, M. L. S.; Bier, J.; Tropsha, A. Structure Based Alignment and Comparative Molecular Field Analysis of Acetylcholinesterase Inhibitors. *J. Med. Chem.* **1996**, *39*, 5064–5071.
- (33) Rogers, D.; Hopfinger, A. J. Application of Genetic Function Approximation to Quantitative Structure–Activity Relationships and Quantitative Structure–Property Relationships. *J. Chem. Inf. Comput. Sci.* **1994**, *34*, 854–866.
- (34) Trinajstić, N. *Chemical Graph Theory*; CRC Press: Boca Raton, FL, 1983; Vol. I, II.
- (35) Hansen, P. J.; Jurs, P. C. Chemical Applications of Graph Theory II: Isomer Enumeration. *J. Chem. Educ.* **1988**, *65*, 574.
- (36) Kubinyi, H. Variable Selection in QSAR Studies. I. An Evolutionary Algorithm. *Quant. Struct.-Act. Relat.* **1994**, *13*, 285–294.
- (37) Sutter, J. M.; Dixon, S. L.; Jurs, P. C. Automated Descriptor Selection for Quantitative Structure–Activity Relationships Using Generalized Simulated Annealing. *J. Chem. Inf. Comput. Sci.* **1995**, *35*, 77–84.
- (38) Fogel, D. B. Applying Evolutionary Programming to Selected Traveling Salesman Problems. *Cybern. Syst. (USA)* **1993**, *24*, 27–36.
- (39) Fogel, D. B.; Fogel, L. J.; Porto, V. W. *Evolutionary Methods for Training Neural Networks*; IEEE Conference on Neural Networks for Ocean Engineering (Catal. No. 91CH3064-3); IEEE, 1991; pp 317–327.
- (40) Goldberg, D. E. *Genetic Algorithm in Search, Optimization, and Machine Learning*; Addison-Wesley: Reading, MA, 1989.
- (41) Forrest, S. Genetic Algorithms: Principles of Natural Selection Applied to Computation. *Science* **1993**, *261*, 872–878.
- (42) Bohachevsky, I. O.; Johnson, M. E.; Stein, M. L. Generalized Simulated Annealing for Function Optimization. *Technometrics* **1986**, *28*, 209–217.
- (43) Kalivas, J. H., Generalized Simulated Annealing for Calibration Sample Selection from an Existing Set and Orthogonization of Undesigned Experiments. *J. Chemomet.* **1991**, *5*, 37–48.
- (44) Iorio, L. C.; Barnett, A.; Leitz, F. H.; Houser, V. P.; Korduba, C. A. SCH23390, a potential benzazepine antipsychotic with unique interactions on dopaminergic systems. *J. Pharmacol. Exp. Ther.* **1983**, *226*, 462–468.
- (45) Iorio, L. C.; Barnett, A.; Billard, W.; Gold, E. H. Benzazepines: structure–activity relationships between D₁ receptor blockade and selected pharmacological effects. In *Neurobiology of Central D1-Dopamine Receptors*; Creese, I., Breese, G. R., Eds.; Plenum Press: New York, 1986; pp 1–14.
- (46) Tice, M. A.; Hashemi, T.; Taylor, L. A.; Duffy, R. A.; McQuade, R. D. Characterization of the binding of SCH39166 to the five cloned dopamine receptor subtypes. *Pharmacol. Biochem. Behav.* **1994**, *49*, 567–571.
- (47) Ghosh, D.; Snyder, S. E.; Watts, V. J.; Mailman, R. B.; Nichols, D. E. 8,9-Dihydroxy-2,3,7,11b-tetrahydro-1H-naph[1,2,3-de]isoquinoline: a potent full dopamine D₁ agonist containing a rigid β -phenyl dopamine pharmacophore. *J. Med. Chem.* **1996**, *39*, 549–555.
- (48) *Sybyl User's Manual Version 6.2*; Tripos, Inc.: St. Louis, MO, 1995.
- (49) Miller, D. D. Steric aspects of dopaminergic drugs. *Fed. Proc.* **1978**, *37*, 2392–2395.
- (50) Strange, P. G. The binding of agonists and antagonists to dopamine receptors. *Biochem. Soc. Trans.* **1996**, *24*, 188–192.
- (51) Berger, J. G.; Chang, W. K.; Clader, J. W.; Hou, D.; Chipkin, R. E.; McPhail, A. T. Synthesis and receptor affinities of some conformationally restricted analogues of the dopamine D₁ selective ligand (5*R*)-8-chloro-2,3,4,5-tetrahydro-3-methyl-5-phenyl-1H-3-benzazepin-7-ol. *J. Med. Chem.* **1989**, *32*, 1913–1921.
- (52) Shah, J. H.; Kline, R. H.; Geter-Douglass, B.; Izenwasser, S.; Witkin, J. M.; Newman, A. H. (\pm)-3-[4'-(N,N-dimethylamino)-cinnamyl]benzazepine analogues: novel dopamine D₁ receptor antagonists. *J. Med. Chem.* **1996**, *39*, 3423–3428.
- (53) Pettersson, I.; Gundertofte, K.; Palm, J.; Liljefors, T. A study on the contribution of the 1-phenyl substituent to the molecular electrostatic potentials of some benzazepines in relation to selective dopamine D-1 receptor activity. *J. Med. Chem.* **1992**, *35*, 502–507.
- (54) Pettersson, I.; Liljefors, T.; Bogeso, K. Conformational analysis and structure–activity relationships of selective dopamine D-1 receptor agonists and antagonists of the benzazepine series. *J. Med. Chem.* **1990**, *33*, 2197–2204.
- (55) Tropsha, A.; Cho, S. J. Cross-Validated R² Guided Region Selection for CoMFA Studies. In Kubinyi, H., Folkers, G., Martin, Y. C., Eds.; *3D QSAR in Drug Design*; Kluwer Academic Publishers: Dordrecht, The Netherlands, 1998; Vol. III, pp 57–69.
- (56) *MOLCONN-X version 2.0*, Hall Associates Consulting: Quincy, MA.
- (57) Iorio, L. C.; Barnett, A.; Billard, W.; Gold, E. H. Benzazepines: structure–activity relationships between D₁ receptor blockade and selected pharmacological effects. *Adv. Exp. Med. Biol.* **1986**, *204*, 1–14.
- (58) Shah, J. H.; Izenwasser, S.; Geter-Douglass, B.; Witkin, J. M.; Newman, A. H. (\pm)-(N-alkylamino)benzazepine analogues: novel dopamine D₁ receptor antagonists. *J. Med. Chem.* **1995**, *38*, 4284–4293.